Investigation of Cyclic Variations of IMEP Under Idling Operation in Spark Ignition Engines

Sung Bin Han*
Department of Mechanical Engineering, Induk Institute of Technology

Cyclic variability limits the range of operating conditions of spark ignition engines, especially under lean and highly diluted operation conditions. The cyclic combustion variations can be characterized by pressure parameters, combustion related parameters, and flame-front related parameters. The coefficient of variation (COV) in indicated mean effective pressure (IMEP) defines the cyclic variability in indicated work per cycle.

Key Words : Coefficient of Variation, Cyclic Variations, Idling, Indicated Mean Effective Pressure, Lowest Normalized Value, Standard Deviation

Nomenclature

c_p : Specific heat at constant pressure
c_v : Specific heat at constant volume
m : Mass of gas in cylinder
T : Mean charge temperature
T' : Crevice gas temperature
T_w : Wall temperature
V_{cr} : Crevice volume
γ : Ratio of specific heats for gas
γ' : Ratio of specific heats for crevice gas
δW : Work done by piston
dU_s : Change in sensible energy from reactants to products
δQ_{ch} : Chemical energy release by combustion
δQ_{ht} : Heat transfer to the chamber walls
$\sum h_i dm_i$: Mass flow across the system boundary

1. Introduction

Much effort has been dedicated to extend the limit of lean burn operation to improve fuel efficiency and reduce exhaust gas emissions from spark ignition engines. The limit is imposed by increased cyclic variation in the combustion intensity which reduces driveability. The effect is usually quantified through the coefficient of variation (COV) of the indicated mean effective pressure (IMEP) (Kiyoshi et al., 1997). Indicated mean effective pressure is an important and fundamental engine performance variable which is used extensively in engine development work.

Cycle-to-cycle combustion variability in spark-ignition engines limits the use of lean mixtures and lower idle speeds because of increased emission and poor engine stability. The causes of the cycle-to-cycle variations are summarized in papers (Ozdor et al., 1994). Although the causes of cycle-to-cycle variability have been identified, there has been difficulty in quantifying these effects. Detailed experimental investigation is difficult. Consequently it is not clear which factor is the most important in the combustion variations (Han and Chung, 1998). One way to examine this problem is through use of a computer simulation (Shen et al., 1994; 1996).

Pischinger and Heywood (1990) found that the cyclic variation of flame propagation near the spark plug influences the amount of heat release at the spark plug gap and this greatly influences the so-called rapid burn angle. Brown et al. (1996) investigated the relationship between the initial speed of combustion and IMEP variation in an experiment which minimized the effect of residual gases. However, Robinet et al. (1997) did

* **E-mail** : sungbinhan@mail.induk.ac.kr
TEL : +82-2-901-7635 ; **FAX** : +82-2-901-7630
Department of Mechanical Engineering, Induk Institute of Technology, San 76 Wolgye-dong, Nowon-gu, Seoul 139-749, Korea. (Manuscript **Received** February 3, 2000; **Revised** June 30, 2000)

not find a good relationship between the IMEP and the direction and expansion speed of the initial flame kernel.

Recently, Hoard and Rehagen (1997) proposed one other means of characterizing cycle-to-cycle variations, the lowest normalized value (LNV). The purpose of this parameter is to assess the misfire tendency of an engine. Tests have shown that LNV correlates well with driver's subjective rating of engine smoothness. Numerical calculations have enabled prediction of the flows inside cylinders, and several studies have reported variations in initial stage of combustion phase due to variations in heat transfer at the spark plug. Through simultaneous laser doppler velocimeter and ionization probe measurements in an engine, some researchers found a strong correlation between the cycle-to-cycle variations in turbulence intensity ahead of the flame and flame arrival time at the LDV probe volume, suggesting that fluctuations in the bulk turbulence intensity ahead of the flame cause variations in burn rate during the main combustion phase (Meyer et al., 1993; Hinze, 1993; 1977).

The objective of this paper is to clarify the sources of cycle-to-cycle combustion variability in a spark ignition engine at idling by varying spark timing operating conditions.

2. Experimental Method

2.1 Engine setup and operating conditions

One characteristic of the cycle-to-cycle variability in an engine is that it is sensitive to operating condition. Therefore, in any effort to study cyclic variations, it is imperative to control the engine operating condition.

Table 1 shows the relevant characteristics of the engine used in this work. The engine has a pentroof head with a centrally-located spark plug. The engine was modified to operate on a single cylinder to avoid multiple cylinder interactions. Thus, fuel is injected and a spark ignition is supplied to only one cylinder, and the intake and exhaust runners of the firing cylinder are isolated.

The engine was coupled to a dynamometer, which was used to maintain the engine speed at

Table 1 Specification of engine used

Engine Type	4-cylinder, 4 valve/cylinder, dual overhead cam
Displacement/cylinder	499.6 cc
Bore×Stroke	86×86 mm
Number of Cylinder	4
Compression Ratio	9.5
Intake Valve	Open 13° BTDC Close 55° ABDC
Exhaust Valve	Open 57° BTDC Close 3° ATDC
Valve overlap	16°

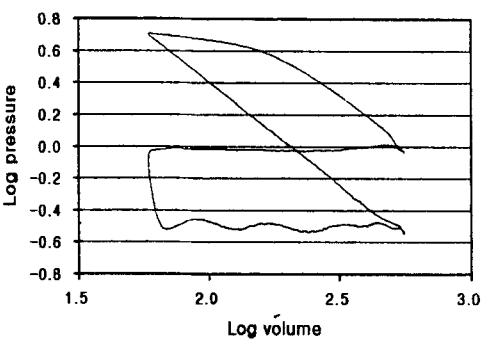

Fig. 1 Log P vs. LogV plot of pressure data with MAP=0.32 bar

800 RPM for all experiments. The coolant temperature was kept around 80℃, and sump oil temperature was kept around 75℃. However, it was not possible to control the inlet air temperature, which varied within a range of 25℃ to 30℃. Cylinder pressure was measured with a Kistler 6051B piezoelectric pressure transducer. The transducer was connected to a Kistler model 5004 dual mode charge amplifier. The voltage output of the amplifier was sampled by a PC-based data acquisition system using a Data Translation A/D converter DT2828. Pressure data were taken at one crank angle interval by using a 360 pulse/revolution optical shaft encoder as an external trigger. The shaft encoder also provided a reference pulse for bottom center.

Figure 1 shows a logarithmic plot of pressure versus volume for an average pressure trace with the inlet manifold pressure at 0.32 bar.

Table 2 The operating condition selected

Engine speed	800 RPM
Inlet manifold pressure	0.32 bar
Inlet air temperature	299 K
Air/fuel equivalence ratio	1.0
Air mass flow rate	0.5998 g/s
Gross IMEP	1.55 bar
Spark timing	15° BTDC

Table 2 shows the operating condition selected. The spark timing and speed were used to the specified values by the test engine for the idle condition. The air/fuel equivalence ratio was kept 1.0 because the engine normally operates with a three-way catalyst, requiring stoichiometric operation. The inlet manifold pressure was adjusted to give an average gross IMEP of 1.55 bar, which typical for an idle condition. All experiments were performed after the engine at a fully warmed-up state.

2.2 Energy release burn-rate model

In order to analyse cyclic variations in the test engine, the fluctuation of burn parameters (e.g. fnel, air, residual mass) are used. These burn parameters are determined on a cycle-to-cycle basis through analysis of the engine pressure data. The burn rate analysis program that was used in the analysis of the data is described in detail by Cheng and Heywood (1993). An ideal set of burn parameters would characterize combustion completely, from start to finish, and difine the total amount of energy released. Also, the burn parameters should be easy to determine from the cylinder pressure data.

Cylinder-pressure based combustion analysis provides combustion process understandable for a combustion process researcher.

To derive the energy release burn-rate, consider the first law of thermodynamics applied to the gas inside the cylinder.

$$\delta Q_{ch}=dU_s+\delta W+\sum h_i dm_i+\delta Q_{ht} \quad (1)$$

The sensible energy can be represented by

$$dU_s=mc_v(T)dT+u(T)dm \quad (2)$$

The piston work is simply given by pressure multiplied by the change of cylinder volume by

$$\delta W=pdV \quad (3)$$

The mass flux across the system boundary is given by two terms:

$$\sum h_i dm_i=h_{inj}dm_f+h'dm_{cr} \quad (4)$$

where the first term describes the energy flow due to fuel injection whereas the second term accounts for the effect of flow into and out of crevices.

The ideal gas law states

$$Vdp+pdV=R(Tdm+mdT) \quad (5)$$

In the burn rate analysis, γ is approximated by a function of temperature by

$$\gamma=a+bT \quad (6)$$

where $\frac{c_v}{R}=\frac{1}{\gamma-1}$

By substituting Eqs. (2) to (6) into (1) and expressing the energy release rate in terms of crank angle provides us with the function form of the burn rate expression:

$$\frac{\delta Q_{ch}}{d\theta}=\frac{\gamma}{\gamma-1}p\frac{dV}{d\theta}+\frac{1}{\gamma-1}V\frac{dp}{d\theta}+V_{cr}\left[\frac{T'}{T_w}+\frac{T}{T_w(\gamma-1)}+\frac{1}{bT_w}\ln\left(\frac{\gamma-1}{\gamma'-1}\right)\right]\frac{dp}{d\theta}+\frac{dQ_{ht}}{d\theta} \quad (7)$$

where $\delta Q_{ht}=Ah_c(T-T_w)$. (8)

The heat loss from the cylinder gas to the cylinder wall is given by Eq. (8). The heat transfer coefficient is given by Wochini's correlation with a minor modification.

3. Results and Discussions

Figure 2 shows the mass fraction burned in a number of cycles for various IMEP values under idle conditions. Figure 3 shows the maximum mass fraction burned in each case. The maximum mass fraction burned is the normalized value with respect to the value for 250 cycles. The maximum value of the mass fraction burned at the spark timing of 25 BTDC recorded the largest value. The minimum value of the mass fraction burned

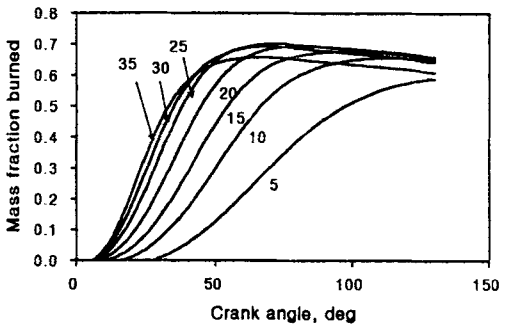

Fig. 2 Mass fraction burned vs. crank angle for spark timings

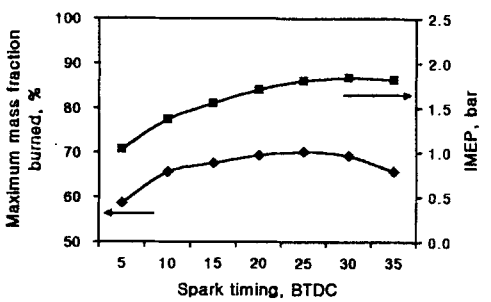

Fig. 3 Maximum mass fraction burned and IMEP vs. spark timings

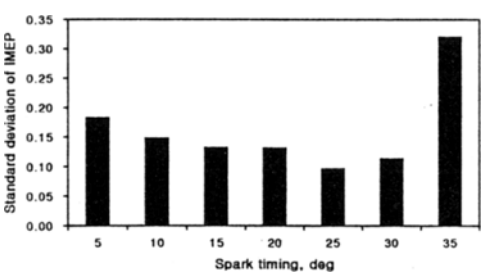

Fig. 4 Standard deviation of IMEP vs spark timing

was about 59% at the spark timing of 5 BTDC. The figure shows that, as the IMEP value is increased, the speed of initial combustion becomes shorter and the mass fraction burned increases. The initial combustion speed is defined as the crank angle interval between spark discharge and the time at which 2% of the mass burned.

Figure 4 shows the standard deviation of IMEP against spark timing for 250 cycles. The test engine has the lowest standard deviation of IMEP at 25 BTDC. This is due to the rapid increase in residual fraction and reduction in charge density

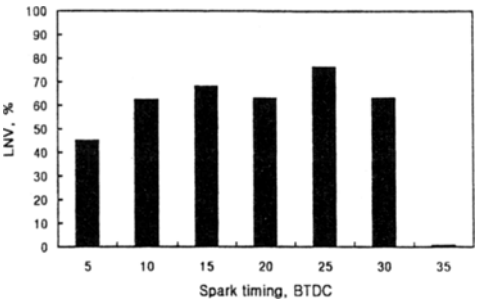

Fig. 5 Lowest normalized value vs. spark timings

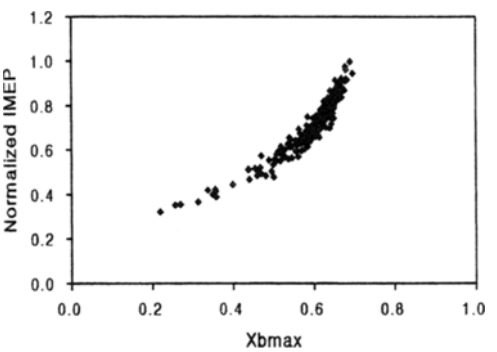

Fig. 6 Normalized IMEP vs. maximum mass fraction burned at 5° BTDC

as the engine is throttled to reduce load. This figure shows that some engines have worse idle stability than the best engines at any given IMEP level.

Figure 5 shows the lowest normalized value (LNV) on the spark timing. LNV is defined as

$$LNV(\%)=\frac{IMEP_{MIN}\times 100}{\overline{IMEP}}$$

where $IMEP_{min}$ is the minimum IMEP value in the data set, and $\overline{IMEP}$ is the mean IMEP of the data set. This value is plotted for the spark sweep in Figure 5. Also, Hoard and Rehagen (1997) suggest that an appropriate value for the lower limit of LNV is 75%. As the figure shows, the experimental engine only matches that criterion at the 25° BTDC spark timing. Extensive empirical experience with combustion parameters and vehicle development has confirmed the results of the earlier experiment.

Figure 6 shows the relationship between the IMEP and maximum mass fraction burned at measured on 250 cycles at 5° BTDC, i. e., the

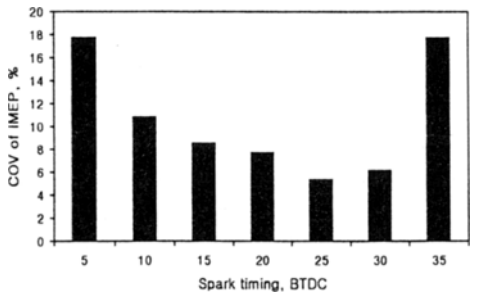

Fig. 7 Coefficient of variation of IMEP vs. spark timings

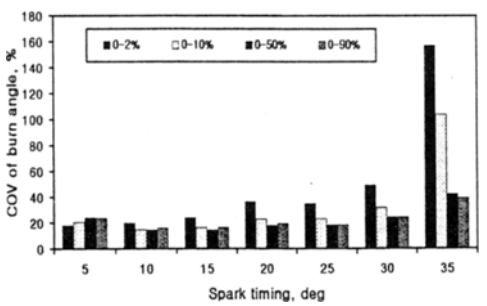

Fig. 8 Coefficient of variation of burn angle vs. spark timings

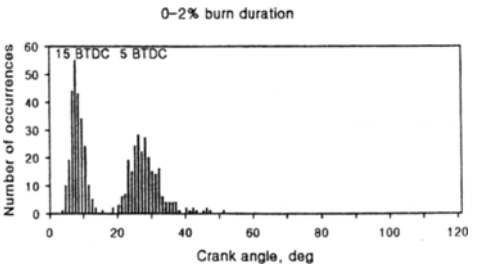

Fig. 9 Number of occurrences vs. crank angle for 0-2% burn duration at 5° BTDC and 15° BTDC spark timings

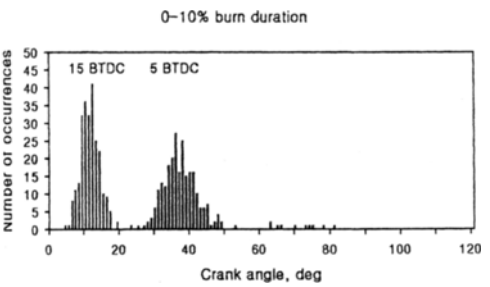

Fig. 10 Number of occurrences vs. crank angle for 0-10% burn duration at 5° BTDC and 15° BTDC spark timings

stable operating limit. The IMEP values for each cycle were normalized by the maximum IMEP value. The figure shows that as expected there is a broad increase in the normalized IMEP with increasing the maximum mass fraction burned. However there is a large scatter between the values of mass fraction burned and those of IMEP, suggesting that heat energy is not converted to mechanical work efficiently.

Figure 7 shows the influence of combustion phasing on the coefficient of variation (COV) of IMEP. COV is the standard deviation in IMEP divided by the mean IMEP.

$$COV_{IMEP}(\%)=\frac{STD_{IMEP}\times 100}{IMEP}$$

As the spark is advanced, the COV of IMEP goes down because relative changes in combustion phasing have a smaller effect on the IMEP, as the spark timing indicated. However, for the two most advanced cases, the COV begins to increase again, probably because the lower temperature at the time of spark is adversely affecting ignition. Note that the COV of IMEP at the idle spark timing is slightly under 10% which is typically considered the limiting point of combustion variability.

Figure 8 shows the COV of burn angle as a function of spark timing with 0-2%, 0-10%, 0-50%, 0-90%, and 10-90% burn angles. The COV of burn angle shows a minimum value at the spark timing 5° BTDC, and the COV of burn angle increases as spark timing is advanced.

Figures 9~12 show the number of occurrences versus spark timing for 0-2%, 0-10%, 0-50%, 0-90%, and 10-90% burn angles at 5 BTDC and 15 BTDC, respectively. The early burn period is characterized by the 0-10% burn angle, also known as the flame development angle. It represents the crank angle interval between spark and the time when 10% percent of the charge mass has been burned. This is often taken as a measure of the time it takes to achieve a fully developed turbulent flame in the cycle. By the time 10% of the charge mass is burned, the flame may be as large as 30% of the total combustion chamber

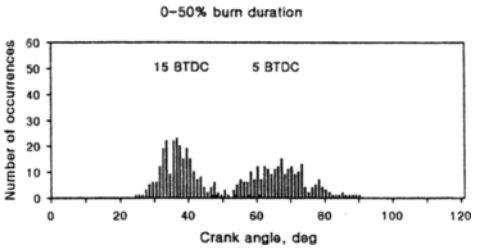

Fig. 11 Number of occurrences vs. crank angle for 0-50% burn duration at 5° BTDC and 15° BTDC spark timings

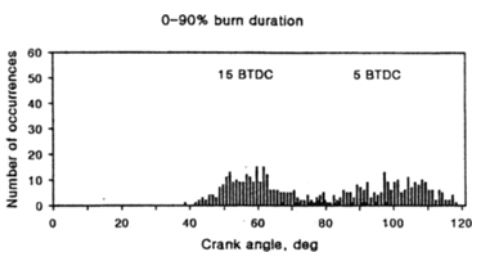

Fig. 12 Number of occurrences vs. crank angle for 0-90% burn duration at 5° BTDC and 15° BTDC spark timings

volume. Thus, the 0-2% burn angle may be preferable when the combustion period of interest is early flame development. However, the resolution of the burn rate analysis was insufficient for detecting changes in 0-2% burn angle between perturbed and non-perturbed cycles. The 0-50% burn angle may be considered an approximate measure of the time it takes the flame to develop from spark to the peak mass burning rate. The 10-50% burn angle is the earlier —and faster—part of the turbulent flame propagation, representing a significant part of the total rapid burning angle. This portion of the combustion process is important from a phasing standpoint: The location of the 50% burn angle may be used as an indicator of combustion phasing with respect to the optimum. Typically, the peak mass burning rate occurs within a few crank angle degrees of the 50% burn angle; thus, from this time onward combustion is slowing down. The burn speed after this point has a smaller influence on IMEP since it is retarded with respect to the expansion stroke. The burned gas is substantially less dense than the unburned mixture. Therefore, by the time 90% of the fuel mass has been burned, almost the entire combustion chamber volume has been engulfed by the burned gas.

4. Concluding Remarks

In this paper, to analyse the cyclic variation in spark ignition engine at idle, a methodology was developed whereby the input variations in air mass, fuel mass, and residual mass could be identified from variations in the output burn parameters. The results obtained are as follows.

(1) Experimental and empirical data suggest that the COV of IMEP and burn angles and LNV levels for acceptable idle quality are fairly similar for a various engines. The COV of burn angle shows a minimum value at the spark timing 5° BTDC where maximum COV of IMEP appears, and the COV of burn angle increases as spark timing is advanced.

(2) As the spark is advanced, the COV of IMEP goes down because relative changes in combustion phasing have a smaller effect on the IMEP. However, for the two most advanced cases at the spark timing 35° BTDC, the COV of IMEP begins to increase again.

Acknowledgement

This study has been supported in part, by Induk Institute of Technology in Seoul, Korea.

References

Brown, A. G., Stone, C. R. and Beckwith P., 1996, "Cycle-by-Cycle Variation in Spark Ignition Engine Combustion-Part Ⅰ: Flame Speed and Combustion Measurements and a Simplified Turbulent Combustion Model," *SAE* Paper 960612.

Cheung, H. M. and Heywood, J. B., 1993, "Evaluation of a One-Zone Burn-Rate Analysis Procedure Using Production SI Engine Pressure Data," *SAE* paper 932749.

Cheung, H. M., 1993, "A Practical Burn Rate Analysis for Use in Engine Development and Design," MIT Thesis.

Han, S. B., and Chung, Y. J., 1998, "A Study

on the Effect of Operating Conditions for the Stability at Idle," *KSME International Journal*, Vol. 12, No. 4, pp. 694~700.

Hinze, P. C., 1993, "A Study of Fuel Effects on Early Flame Development in a Spark Ignition Engine," MIT Thesis.

Hinze, P. C., 1997, "Cycle-to-Cycle Combustion Variations in a Spark-Ignition Engine Operating at Idle," MIT Ph. D. Thesis.

Hoard, J. and Rehagen, L., 1997, "Relating Subjective Idle Quality to Engine Combustion," *SAE* Paper 970035.

Kiyoshi, I., Sasaki, T., Urata, Y., Yoshida, K., and Ohno T., 1997, "Investigation of Cyclic Variation of IMEP Under Lean Burn Operation in Spark-Ignition Engine," *SAE* Paper 972830.

Meyer, R., Kubesh, J. T. and Shahed, S. M., 1993, "Simultaneous Application of Optic Spark Plug Probe and Head Gasket Ionization Probe to a Production Engine," *SAE* Paper 930464.

Ozdor, N., Dulger, M. and Sher, E., 1994, "Cyclic Variability in Spark Ignition Engines A Literature Survey," *SAE* Paper 940987.

Pischinger S. and Heywood, J. B., 1990, "How Heat Losses to Spark Plug Electrodes Affect Flame Kernel Development in an SI Engine," *SAE* Paper 900021.

Robinet, C., Andrzejewski, J., and Higelin, P., 1997, "Cycle-to-Cycle Variation Study of an SI Engine Fired by Spark Plug and a Non Conventional Device," *SAE* Paper 972986.

Shen, H., Hinze, P. C. and Heywood, J. B., 1994, "A Model for Flame Initiation and Early Development in SI Engine and its Application to Cycle-to-Cycle Variations," *SAE* Paper 942049.

Shen, H., Hinze, P. C. and Heywood, J. B., 1996, "A Study of Cycle-to-Cycle Variations in SI Engines Using a Modified Quasi-Dimensional Model," *SAE* Paper 961187.